THE GREEN POND OUTLIER OF NEW YORK AND NEW JERSEY; A MESOSTRUCTURAL LABORATORY

JAMES P. MITCHELL,
The Pennington School, Pennington, NJ 08534

RANDALL D. FORSYTHE
Department of Geography and Earth Science, UNCC, Charlotte, NC 28227

INTRODUCTION

Exposures of the folded Silurian and Devonian strata of the Green Pond outlier within the Reading Prong of New Jersey and New York (Fig. 1a.) contain abundant small scale deformation features. These include: slickenfiber faults, en echelon vein arrays, two sets of disjunctive cleavage, and small scale folds. This trip visits a series of outcrops within the outlier that permit a detailed study of the interrelationships and origin of these mesostructures.

Students of structural geology are commonly introduced to small scale (meso) structures classed as being either brittle or ductile. In the Earth, however, brittle deformation is not necessarily restricted to the upper "seismogenic" layer, and ductile deformation likewise is not restricted to the deeper medium to high grade metamorphic levels. Folds that form under moderate confining pressure and low temperatures, often reveals a confusing array of both ductile and brittle mesostructures. The manner in which these ductile and brittle features are related is one of the interesting topics that can be examined on this trip.

The trip also provides students an opportunity to understand some of the dynamic or stress conditions that operate during folding. Published work on folded strata (for discussion see Ramsay, 1967) has generally focussed on the geometric development of folds and its strain-related cleavages or foliations. The array of semi-brittle features that formed along with the cleavage in the Green Pond outlier permits an appreciation of the forces or stresses responsible for folding.

THE GREEN POND OUTLIER

Paleozoic formations in the outlier. Figure 1b shows the principal distribution of the units within the outlier. For simplicity, the ten Silurian and Devonian formations (stratigraphy shown in Fig. 2) are grouped into three lithostratigraphic units (III, IV, and V). These rest with angular discordance over Middle Proterozoic rocks (unit I) in some places but over a thin veneer of Cambrian and Ordovician rocks (unit II) in others (Barnett, 1976; Herman and Mitchell, in press). The 2,400 meters of Silurian and Devonian rocks, that makeup the bulk of the outlier (see Fig. 3) have strong inter-, and intraformational competency differences. Unit III, the Green Pond Formation (Silurian), is equivalent to the Schawangunk Conglomerate of the Valley and Ridge Province (Lewis and Kummel, 1915), and is composed of

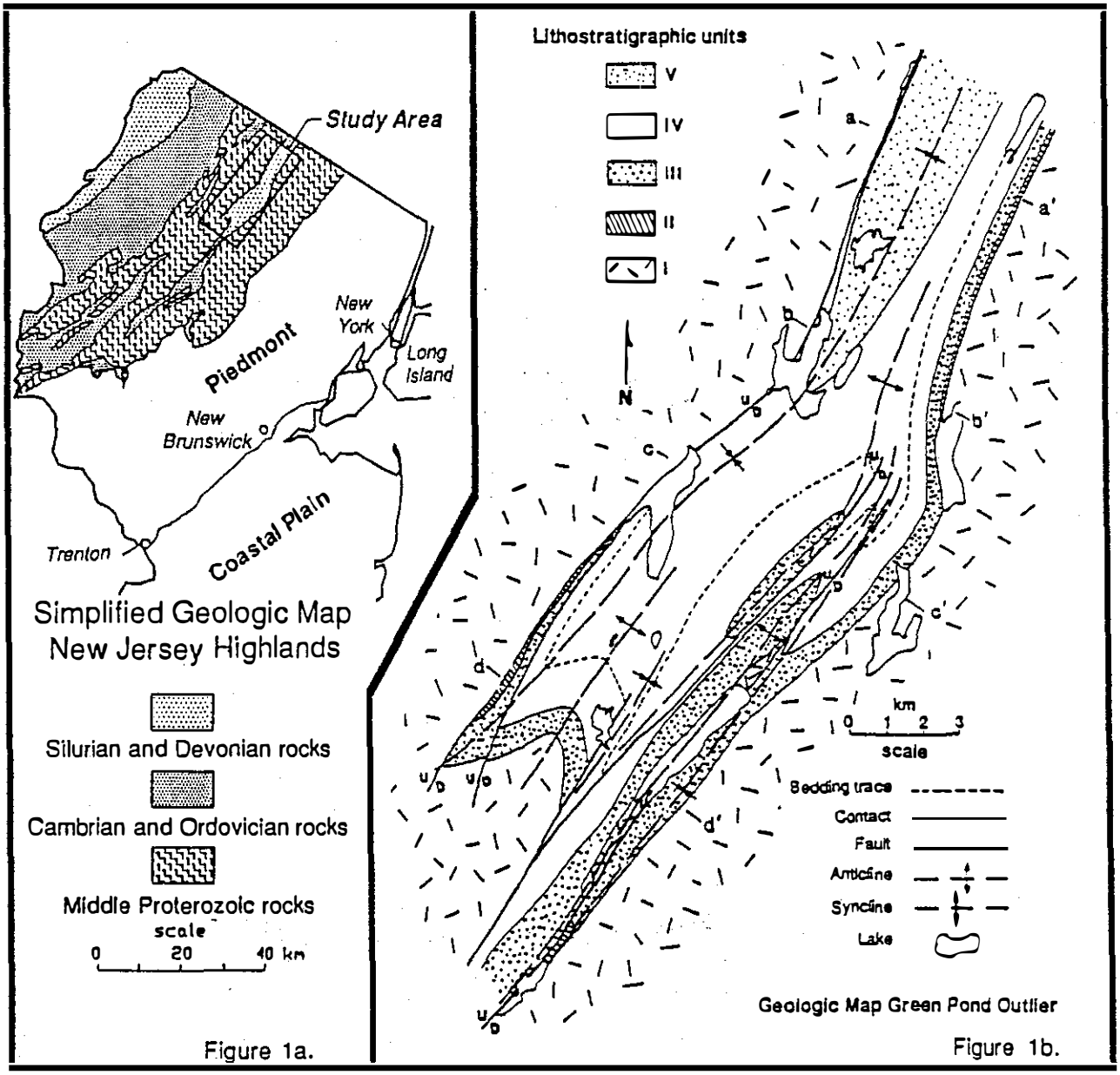

interbedded purple-red conglomerate, cross bedded sandstone and minor siltstone units. The conglomerate and sandstone units are well indurated. They have highly sutured clasts and a siliceous and hematitic cement. The central portions of the sequence, unit IV, contain some of the less competent units, such as the Longwood (Sil.) and Cornwall Shales (Dev.). These units have the best development of disjunctive cleavage, but are not as well exposed in the outlier. The Middle Devonian Skunnemunk Formation (Catskill delta equivalent), is a ridge former, and like the basal Green Pond Formation is also well indurated, though the former tends to break around the grains when fractured.

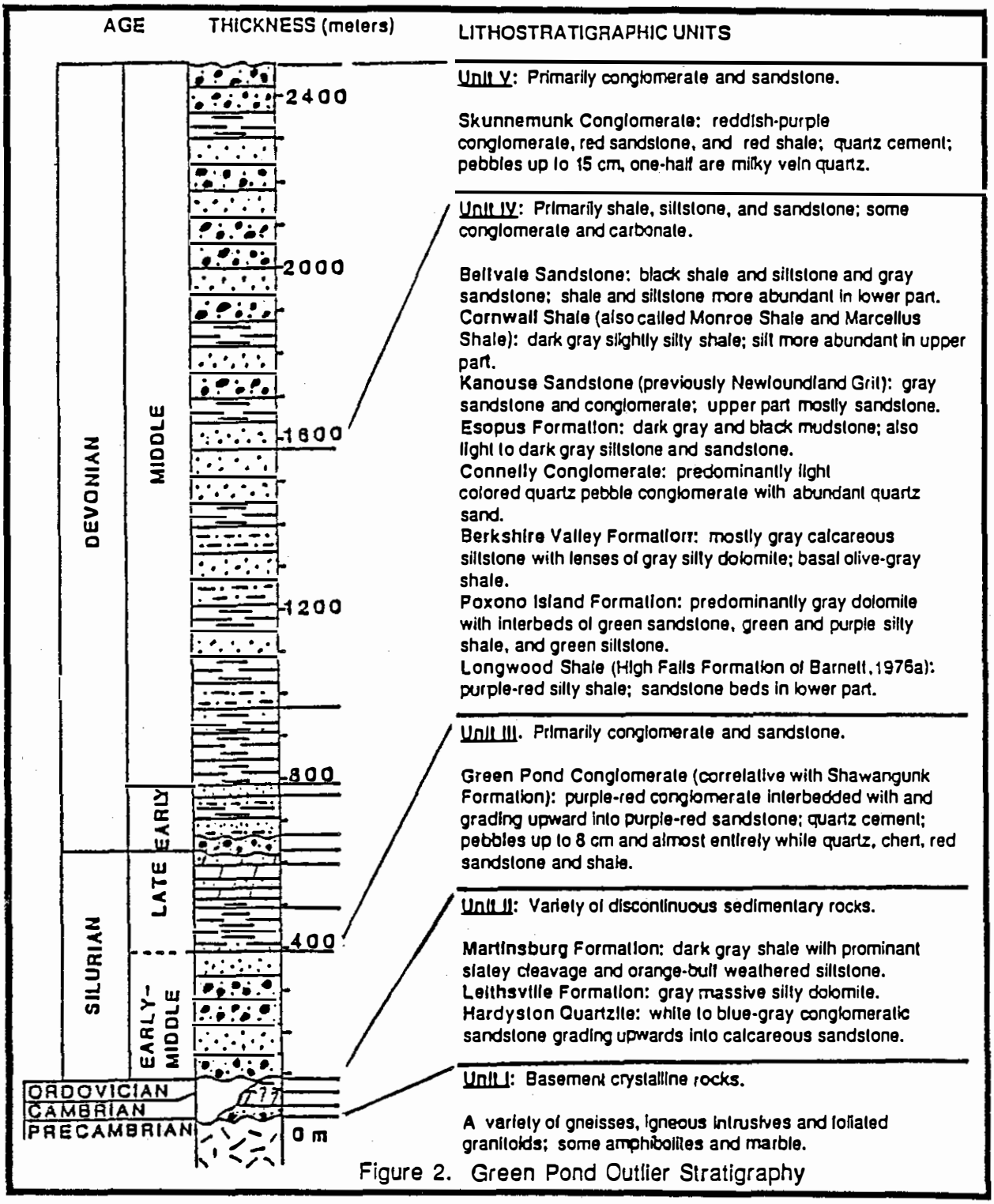

Figure 2. Green Pond Outlier Stratigraphy

Structure of the Green Pond outlier. The outlier is defined by a series of northeast trending fold structures that have been down-faulted within the Reading Prong. (Fig. 1b, 4a). The large scale folds defined by the more competent units (III & V) and perhaps mechanically controlled by the basal contact with the underlying Proterozoic crystalline rocks have relatively planar limbs and sharp well defined hinges suggestive of a kink fold geometry. Within these large scale structures occur smaller amplitude open to tight folds that have curved parallel geometries. Most hinges plunge gently to the

northeast but others are doubly plunging. In New York State the outlier is defined by one large tightly folded asymmetric syncline with a steeply dipping to slightly overturned eastern limb. It is fault bounded to the northwest and southeast. Southwestwards in New Jersey the outlier's structural form expands to include three smaller amplitude folds. Each of the fold structures is fault-bounded, with the exception of the eastern margin of the outlier in our study area where the Green Pond Formation is thought to rest in depositional contact with both lower Paleozoic and Proterozoic rocks (Kummel and Weller, 1902; Barnett, 1976). Faults trend parallel to the axial traces of folds and tend to be associated with the eastern limb of anticlines. Fault attitudes and displacement histories have been variably interpreted over the years (Kummel and Weller, 1902, Lewis and Kummel, 1910 & 1915; Ratcliffe, 1980). However, the most recent mapping (Herman and Mitchell, in press) has identified high angle reverse faulting in the central part of the outlier and conjugate reverse faults to the southwest around Dover, New Jersey.

MESOSTRUCTURES

Small scale structures, believed to have been developed in addition to the large scale folding and faulting of the outlier are: two sets of cleavages, small scale folds, en echelon vein arrays (EVA's) and slickenfiber faults (SFF's) (Mitchell and Forsythe, 1988).

Cleavages. Within the outlier cleavages are best developed in the more argillaceous formations such as the Longwood and Cornwall Shales. In most localities a slaty to spaced cleavage can be observed in the shaly and silty units that is subparallel to the axial surfaces of the local fold structures. However, in addition to the axially planar cleavage, several localities reveal a cleavage of slaty, pressure solution, or crenulation type, that trends obliquely across the fold structures with attitudes ranging from N 60 E to E-W. In a few places (e.g., Stop 3) both cleavages are found together and document an interesting shift or noncoaxial character in the directions of 'finite' shortening accompaning their development (discussed below).

En echelon vein arrays (EVA's). (terminology of Beach, 1975) These are also known by some as en echelon tension gashes (Shainin, 1950; Dalziel and Stirwalt, 1975). They are staggered sets of veins that are aligned in one common plane. Examples in Figure 3b, show two of their common geometric and dynamic configurations. Unless they occur in conjugate sets or with other brittle features, it is not obvious whether they are of a specific type. The production of an EVA in a rock is the distortional equivalent to a dilating zone of shear. It is, however, produced by the progressive cracking and infilling of the veins during shearing. Thus these 'shear zones' are regarded as a class of "brittle-ductile" features (Ramsay, 1980b). In the Green Pond outlier, they are most commonly developed in the indurated sandstone and conglomerate layers of units III(Green Pond Formation) and V(Skunnemunk Conglomerate).

Slickenfiber faults (SFF's). (terminology of Wise et al., 1984) These also are features that, in part, form by crack propagation (Durney and Ramsay, 1973; Ramsay, 1980). These are regarded as a subset or special class of faults within which fibrous minerals grow and infill the spaces opened up within the

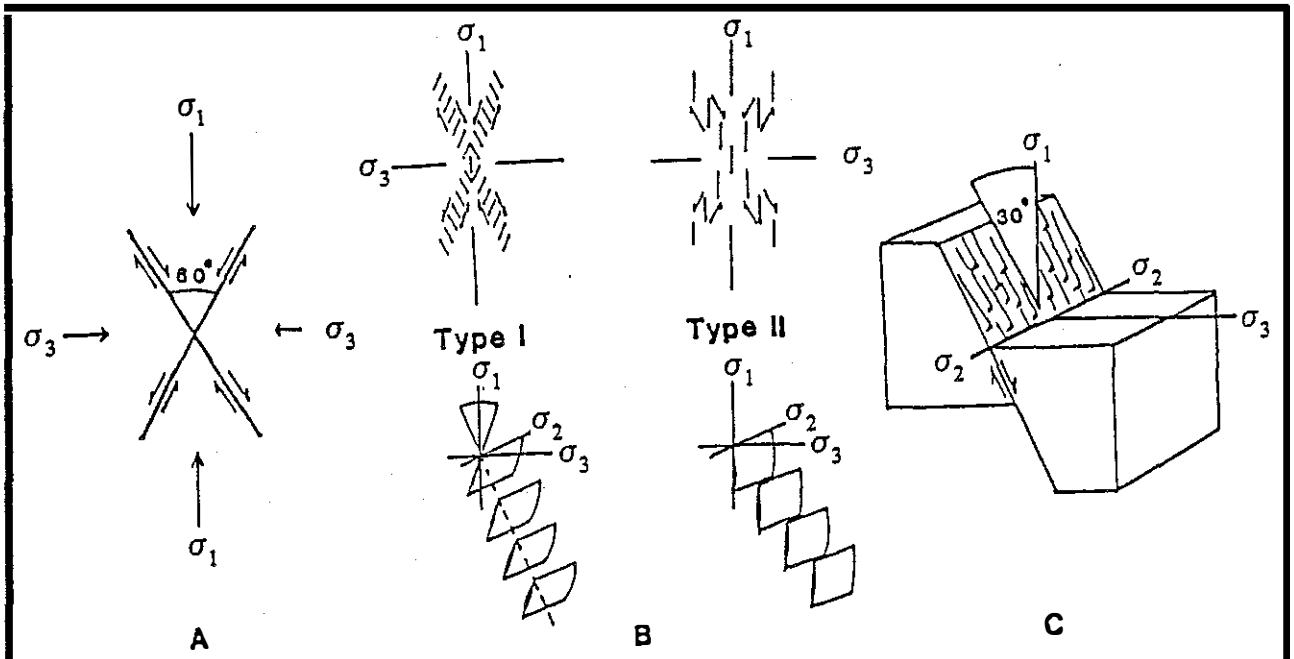

Figure 3. A. general relations between shear failure planes and principal stresses
B. relations between two types of EVA and principal stresses, after Beach, 1975
C. relations between slickenfiber faults and principal stresses.

fault zone during faulting. The fibers tend to connect formerly adjacent points on the opposite walls of the fault. Slickenfiber faults, like the EVA's are developed in the more competent units of the Green Pond outlier. Relations suggest that they develop instead of an EVA due to pre-existing surfaces of weakness in the rock being appropriately oriented for slip. Cross-bedding in the conglomerates and sandstones is commonly a plane of weakness along which SFF's were developed.

STRAIN AND PALEOSTRESS FIELDS

There are important distinctions to be made between the indicators of strain and paleostress in rocks.

Strain Marker. Generally most strain markers are found representative of a finite or long term product of distortion. Cleavage, for example, is commonly thought to be a plane of finite flattening disposed normal to the maximum axis of finite shortening (Ramsay, 1967). Viewed as such, it is a physical product of a protracted history of deformation that can tell us little about the specific flow or distortions occuring at a given instant. Thus strain markers in general provide a restricted or limited view of the deformation history.

Paleostress markers. Most paleostress indicators on the other hand are more like snap shots of the conditions of deformation that existed at various times during the deformation. In general both EVA's and SFF's contain geometric attributes which can be modeled after brittle features observed in the laboratory and which by analogy permit the inference of the orientation (but not magnitude) of ancient stress fields.

Paleostress determinations. Assessments of paleostresses are made with confidence when EVA or SFF features are present in conjugate sets. Such sets have formed the basis of many previous studies (Roering, 1968; Hancock, 1972; Beach, 1975; and Rickard and Rixon, 1983). In each case the direction of maximum compressive stress and incremental axis of greatest shortening bisects the acute angle between intersecting shear zones (Fig. 3). This condition is true for both biaxial and triaxial strains (Hancock, 1985; see Fig. 2). Two types of conjugate EVA geometry (Fig. 6b) have been described by Beach, 1975 (also see Roering, 1968; and Rickard and Rixon, 1983). In type 1 geometry, not all veins are parallel, rather, the veins of one shear parallel the orientation of the complimentary conjugate shear. Consequently in type 1 geometry the bisector of the conjugate EVA zones also bisects the acute angle between each vein and its enveloping shear. Also, a single large vein typically occurs at the intersection of the two shears which parallels the conjugate shears' bisector (Rickard and Rixon, 1983). In type 2 geometry (Fig. 3b) the veins of both shears parallel the conjugate shears' bisector.

In the field, the easiest case for paleodynamic determinations is for conjugate shears. For isolated arrays or SFF features additional considerations are necessary. In the Green Pond outlier, Mitchell and Forsythe (1988) made the following simplifying assumptions:

1) For each **EVA** the maximum principal stress axis bisects the acute angle between an individual vein and the plane containing the vein array for which the individual is a set member (Fig. 3b, type 1). This assumption appears valid since the bulk of our conjugate EVA's are type 1 of Beach (1975).

2) For each **SFF** an approximation of the maximum principal stress is assumed to lie about 30 degrees from the shear surface and in a plane containing the normal to the plane and the fiber lineation observed on the surface of the fault (Fig. 3c). Since two solutions are possible the sense of displacement must be determined from the overlap of the incremental fibers (Durney and Ramsay, 1973) for a unique solution. The 30^{o} angle is measured from the fault surface in a sense compatible with the sense of displacement (e.g. clockwise for right lateral, and counterclockwise for left lateral displacements).

3) For each **EVA** and **SFF** the intermediate principal stress is assumed to lie in the plane of the shear zone and perpendicular to the displacement direction. For EVA's it also parallels the intersection made by each vein with its enclosing array.

DEFORMATION OF THE GREEN POND OUTLIER

Paleostress trends. The results and interpretations of a regional investigation of SFF and EVA from the central portion of the Green Pond outlier were presented by Mitchell and Forsythe (1988). The study included 130 paleostress determinations from SFF's and 200 from EVA's. Approximately 80 EVA's were from conjugate sets. Most of the observations came from exposures of the Green Pond Formation, but 4 localities were located in the Middle Devonian Skunnemunk Formation. The data were grouped into 17 localities (Fig. 4a) that covered 4 southeast dipping fold limbs, 3 northwest dipping fold limbs and 2 hinge zones. The data are reproduced on stereonets in Figure 4b and on rose diagrams for each locality in Figure 5 for SFF and EVA data. The plots document a number of the general findings. First, most SFF'S and EVA'S record vertical S_1 - S_3 planes with S_2 horizontal (S_1, S_2,

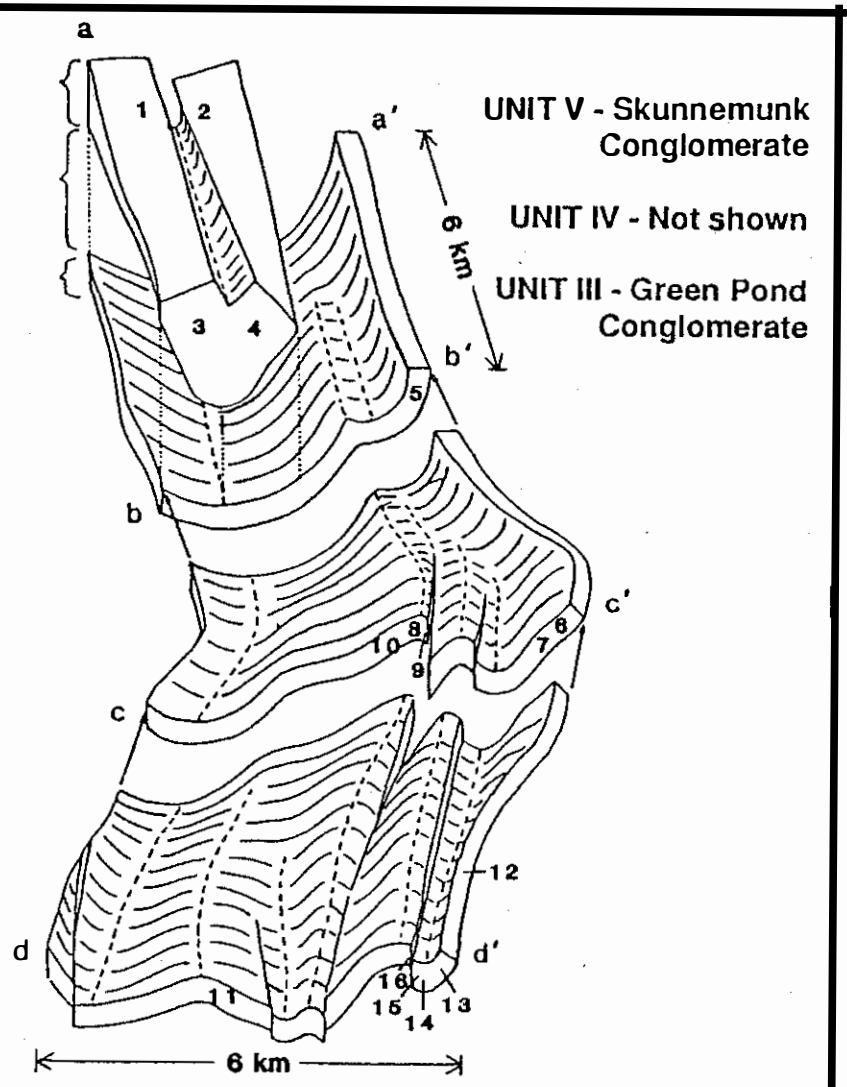

Figure 4a. Perspective drawing of the outlier with data sites

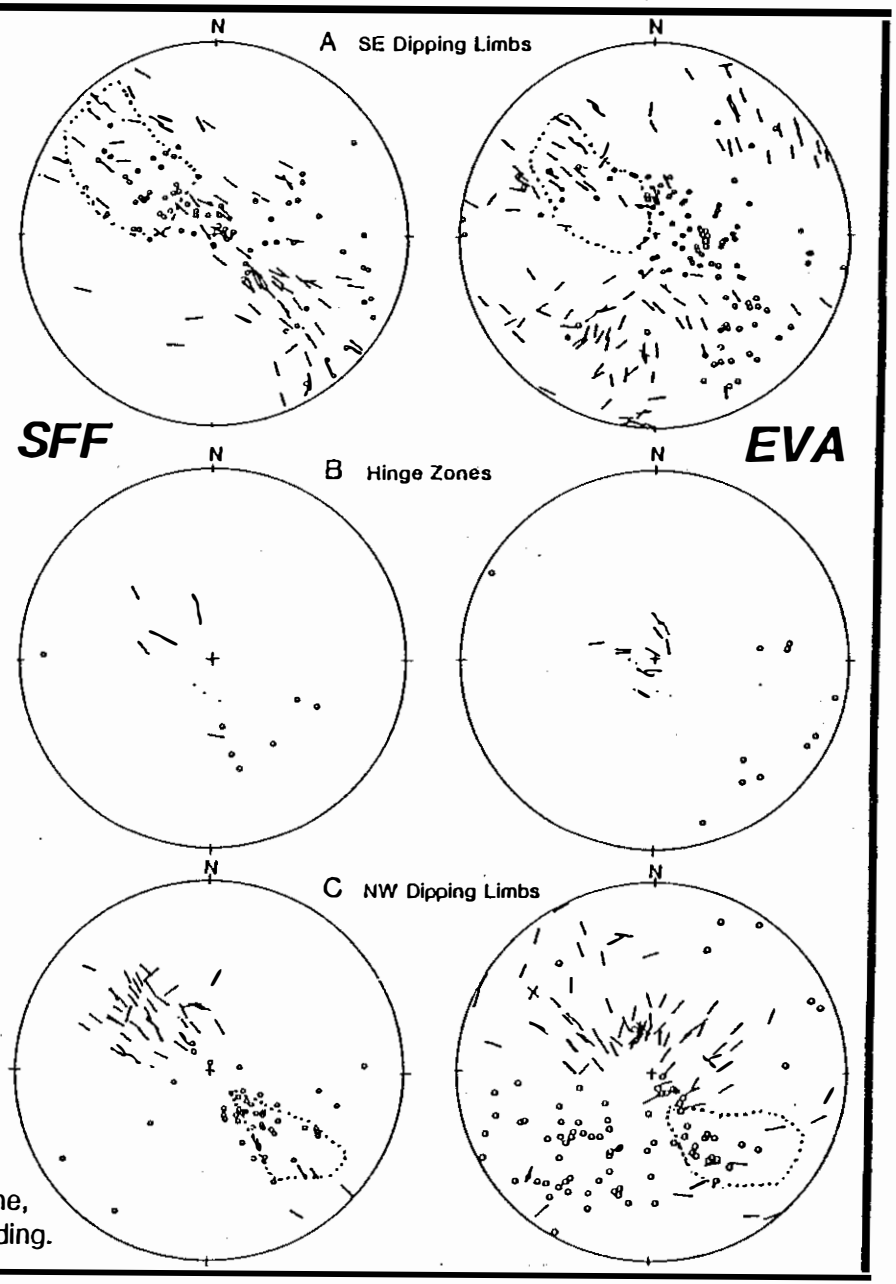

Figure 4b. Plots of max. and min. stress determinations for EVA and SFF. Short lines are max. axes oriented in max.-min. plane, and circles are min. axes. Dotted lines define fields of poles to bedding.

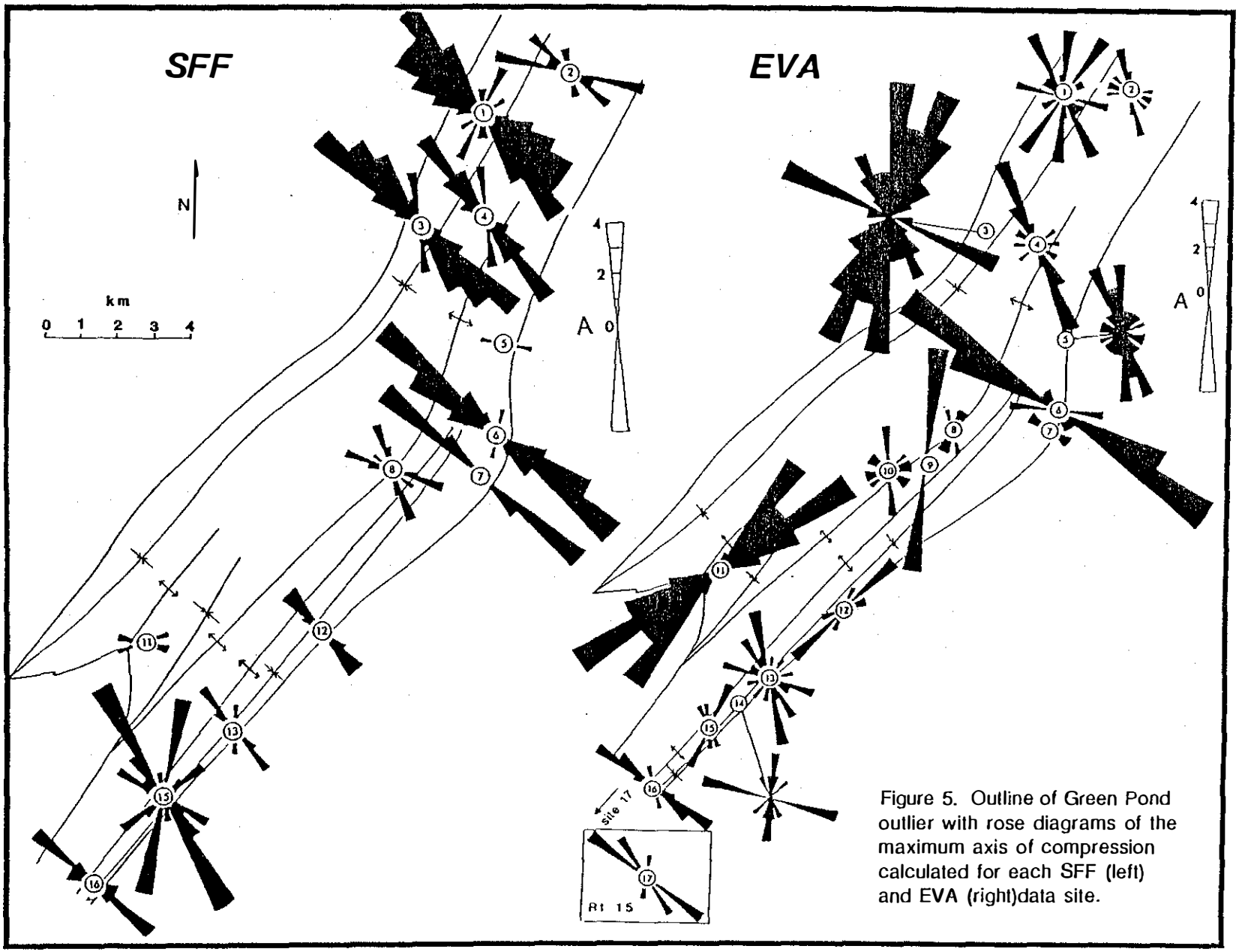

Figure 5. Outline of Green Pond outlier with rose diagrams of the maximum axis of compression calculated for each SFF (left) and EVA (right)data site.

S_3: principal stresses). Second, cumulative rose diagrams for EVA'S and SFF'S indicate that the majority of S_1 axes trend to the NW or SE, essentially at right angles to the fold hinges. Two other modes of S_1 orientations are also present. One trends N-S, the other NE-SW. Third, the SFF data primarily record the dominant NW-SE directed S_1 whereas EVA data have all three modes. Trends for SFF's are much more regionally consistent than those for EVA's, and in addition they show little variation in S_1 trends from different structural positions on the fold structure. However plunges of paleostress axes determined from SFF as well as EVA, do show systematic variations with respect to positions on fold structures. Overall the paleostress data indicated that SFF and EVA have recorded a complex pattern of changing stress conditions in both space and time.

The paleostress data is highly variable. After grouping the data by structural position in the various folds, as well as by general azimuth (of the axis of maximum compression), it is found that much, if not all, of this variability could be accounted for by a combination of two superimposed structural phenomena. The first phenomenon (stage I of Mitchell and Forsythe, 1988) is postulated to be the main phase of folding in the Green Pond outlier under a sub-horizontal NW-SE directed regional maximum compressive stress regime. The second, more illusive, phenomenon (stage II) is thought to have resulted from the rotation of the regional stress field from a NW-SE to a N-S orientation. Under this new field, a phase of noncoaxial shortening took place by the generation of a cross cutting cleavage and numerous additional EVA's that indicate N-S to hinge-parallel maximum compressive stresses.

Stage I (Progressive Buckling). The preponderance of EVA's and SFF's display changes in character and orientation (plunge) that compare favorably with the theoretical computer models of the stress history of folding by Dieterich, 1970 (Figure 6). These models have also compared well to both empirical and other natural folds (Dieterich and Carter, 1969) where there exists significant contrast in the viscosities of the interbedded layers. In the Green Pond outlier variable development of cleavage in the different lithologies, the strong refraction of cleavage from one layer to another, and the general curved parallel fold forms argue for strong inter- and intraformational variations in competency or viscosity during folding. Basically, the argillite and siltstone layers have, through cleavage development, accommodated the buckling

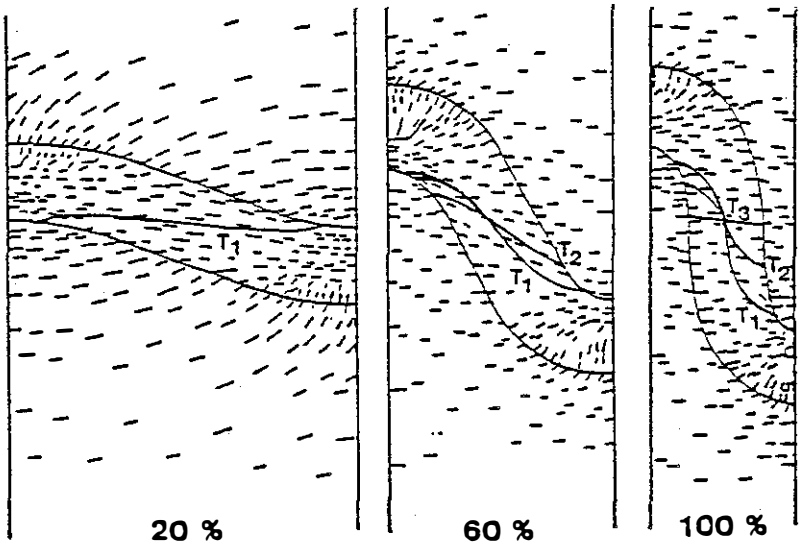

Figure 6. Tracings of maximum principal stress trajectories at three progressive stages of folding based on the computer models of Dieterich and Carter, 1969.

of the more competent sandstone and conglomerate layers. In the theoretical and empirical folding of layers of variable viscosities, it is commonly found that some layer-parallel shortening occurs before appreciable buckling of the higher viscosity layers. As buckling begins there is first a strong guiding of the stresses that keeps the maximum principal axis of compression along the layering. However, as the fold tightens up, the steeply inclined limbs can no longer effectively guide the stresses and the direction of the maximum principal axis returns to take on a position more similar to the external field. The models would argue for three general stages of mesostructural development: an early layer parallel shortening phase, a main buckling phase with the stresses strongly rotated along with bedding, and a late phase with the stresses relaxed in the inclined limbs back to a subhorizontal orientation. These phases are believed to be reflected in the mesostructures of the Green Pond outlier.

Early layer-parallel shortening in the outlier is to be expected to a limited extent because even the resistant conglomerate beds are likely to have had some degree of non-elastic or viscous response to the applied stresses. In the Green Pond outlier most of the slickenfiber faults, and a large percentage of the en echelon vein arrays, indicated paleo-S_1 axes lying at very low angles to bedding (Forsythe and Mitchell, 1988). In addition, several of these EVA's are found bent or folded around small scale folds (Stop 1). The general impression from these relations is that many of the paleostress markers were developed at an early stage in the deformation. Furtherhmore, since buckling reduces the elastic resistance to the applied stress field, it would intuitively follow that nucleation of these brittle ruptures initiated during the threshold stresses that existed in the pre- to early buckling moments. Thus, the first stage of EVA and SFF development in the Green Pond Outlier is postulated to have been represented by an early phase of layer parallel shortening. We suggest as illustrated in Fig. 7, that the preponderance of SFF's that nucleated on the low angle cross beds (mostly west dipping), and EVA's that nucleated in the conjugate orientation, likley accomodated layer parallel shortening in these competent units during the early stages of deformation.

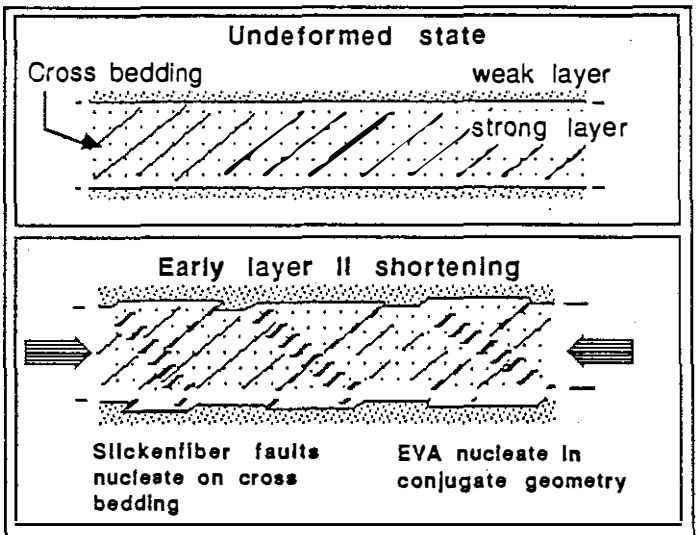

Figure 7. SFF (on cross bedding) and EVA form early conjugate arrays that may have accommodated layer parallel shortening.

As buckling took place, theoretical models of folding would argue for a number of temporal and spatial relationships among mesostructures. The changes to be expected as a function of time (or degree of folding) would best be observed in the limbs of the folds where the rotation of bedding has

progressively changed the orientation of the bed with respect to the regional stress field. During progressive folding the competent or higher viscosity layers, acting as stress guides, rotates the local or intrabed stress axis of maximum compression along with the fold limb away from the subhorizontal regional field. With respect to an internal reference frame (fixed to bedding) the rotation of the stress axis is slightly in the opposite direction. This is because the beds are rotated more than the stresses. With progressive tightening of the fold, the ability of the high viscosity beds to guide the stresses in the limbs of the folds are lost and the local axis of maximum compression 'relaxes' back to a direction closer to the regional or 'far' field orientation. This complex rotational history explains two attributes seen in the Green Pond stage I paleostress data. First, as discussed by Mitchell and Forsythe (1988), it explains the systematic asymmetry in the variations of plunge observed for the maximum principal stress determined from EVA data of east and west dipping limbs. For each limb a gap in plunges was observed in the direction opposite to the dip of the beds (see Figure 12 of Mitchell and Forsythe, 1988). The dispersion and gap in the data is precisely what would be predicted by the combined external and internal rotations described above. Secondly, the rotations can help to explain why conjugate sets of EVA's on a given fold limb appear to have dramatically different forms. Once an EVA is nucleated it represents a plane of weakness that will have a protracted history of development during which limb rotation and folding is occuring. As the stresses shift with respect to bedding, the resolved normal and shear stress components on the conjugate arrays are constantly changing. As illustrated in Figure 8 dextral and sinistral EVA shear zones have internal rotations which will either be compatible (syn-rotational) or incompatible (anti-rotational) with the rotation of the stress axes (using an internal reference frame). Thus, on one limb we predict the early dextral EVA to be the syn-rotational array, while on the other limb the early sinistral EVA is the syn-rotational array. Synrotational EVA's have the plane of vein propagation rotating in a sense similar to the stress field, and the anti-rotational veins in the opposite sense. The anti-rotational EVA's should show pronounced sigmoidal shapes, with multiple or superimposed

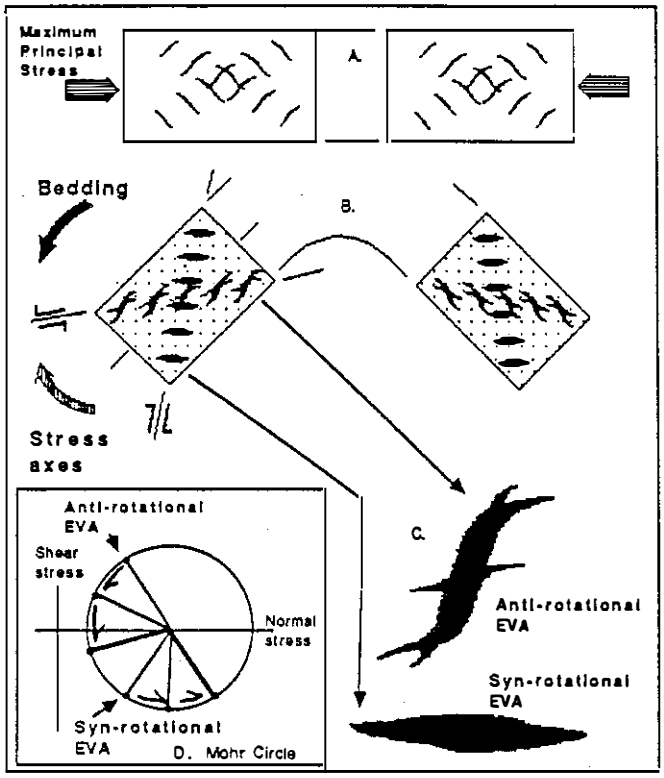

Figure 8. Progressive development of EVA during buckling. A. Early formed conjugate EVA's with thin and planar veins. B. Highly evolved EVA's in advanced stages of buckling that show asymmetry of character as a function of fold limb rotation (with respect to stress axes). C. closeup sketches of the two end-member EVA forms for evolved EVA on fold limbs. D. Mohr Circle illustrating the complex and variable stress histories seen by conjugate pairs of EVA's on fold limbs.

veins, while the syn-rotational EVA's would have more planar forms, and small aspect ratios.

Stage II (Noncoaxial Shortening). This phase is represented by numerous EVA's that indicate N-S to hinge parallel compression, as well as a second cleavage with a rough E-W orientation that trends obliquely across the fold structures. In a few localities (e.g. by Terrace Pond) SFF's have also been found that have multiple orientations of fibers. The superposition of the fibers indicates a similar late stage of N-S oriented regional maximum compression. Thus EVA, cleavage, and limited SFF data, all support a second phase of regional deformation in the outlier under a new N-S regional compressive stress field. Neither the main, stage I, folds nor the axially planar cleavage would have been appropriately oriented to accomodate shortening along this N-S axis. The folds, perhaps like the corrugations in a sheet of metal, would likely have acted as stress guides within this new N-S field. This effect, may in fact explain why there is a significant scatter of Stage II orientations from a N-S to a hinge parallel orientation.

SUMMARY

The abundant development of EVA's and SFF's in the more resistent layers of the Green Pond outlier have provided an opportunity to see how these layers have acted as stress guides throughout the deformation in the outlier, and how the stress fields have changed during the buckling history. The development of an axially planar cleavage in the 'softer' units permits a combined strain and paleostress visualization of the deformation.

Cleavages and folds, while representing long term 'finite' deformation, may not always accomodate the entire deformation. In the Green Pond outlier, as the regional stresses rotated to a new orientation, a second, new cleavage had to form. Therefore, neither the early nor the late cleavage could strictly speaking be said to represent the complete flattening strain in the rock. Each cleavage sees only the strain of its defomation phase. Similarly, the folding has principally accomodated one of two directions of regional shortening. Internally within the folds brittle and ductile structures were both needed to accomodate the deformation. The combination of these structures have given us the unique opportunity to see a combined strain and paleostress record of buckling as well as for the regional superposition of two non-coaxial phases of deformation.

ACKNOWLEDGMENTS

We would like to thank Anna Mitchell and Lisa Chisholm for their help and encouragement. We also thank Gregory Herman, Alexander Gates, and Dennis Weiss for their reviews and comments.

REFERENCES CITED

Barnett, S. G., 1976, Geology of the Paleozoic Rocks of the Green Pond outlier: Geologic Report No. 11, Trenton, New Jersey Geological Survey, 9p.

Beach, A., 1975, The geometry of en-enchelon vein arrays: Tectonophysics, v. 28, p. 245-163.

Dalziel, I. W. D., and Stirwalt, G. L., 1975, Stress history of folding and cleavage development, Baraboo syncline, Wisconsin: Geological Society of America Bulletin, v. 86, p. 1671-1690.

Dieterich, J. H., 1970, Computer experiments on mechanics of finite amplitude folds: Canadian Journal of Earth Sciences, v. 7, p. 467-477.

Dieterich, J. H., and Carter, N. L., 1969, Stress-History of folding: American Journal of Science, v. 267, p. 129-154.

Durney, D. W., and Ramsay, J. G., 1973, Incremental strains measured by syntectonic crystal growths, in: De Jong, K. A. and Scholten, R., eds., Gravity and Tectonics, p. 67-96, Wiley, New York.

Hancock, P. L., 1972, The anaylsis of en-echelon veins: Geology Magazine, v. 109, p. 269-276.

---------, 1985, Brittle microtectonics: principles and practice, Journal of Structural Geology, v. 7, p. 437-457.

Herman, G. C., and Mitchell, J. P., in press, Bedrock Geology of the Green Pond outlier from Dover to Greenwood Lake, New Jersey, New Jersey Geologic Map Series, Map 88-5, 1:24,000 scale, 3 plates, New Jersey Geologic Survey, Trenton, New Jersey.

Kummel, H. B., and Weller, S., 1902, The rocks of the Green Pond mountain region, Annual report of the state geologist for 1901, New Jersey Geological Survey, p. 1-51.

Lewis, J. V., and Kummel, H. B., Geologic Map of New Jersey (1910-1912), Atlas Sheet no. 40, State of New Jersey Department of Conservation and Economic Development, Trenton, New Jersey.

---------, 1915, The Geology of New Jersey: a summary to accompany the Geologic Map (1910-1912), Geol. Survey of New Jersey Bulletin 14, 146 p.

Mitchell, J. P., and Forsythe, R. D., 1988, Late Paleozoic noncoaxial deformation in the Green Pond outlier, New Jersey Highlands, Geol. Soc. Am. Bull., v. 100, p. 45-59.

Ramsay, J. G., 1967, Folding and Fracturing of Rocks, McGraw-Hill, New York, 568 p.

---------, 1980a, The crack and seal mechanism of rock deformation, Nature v. 284, p. 135.

---------, 1980b, Shear zone geometry: a review, Journal of Structural Geology, v. 2, p. 83-99.

Ratcliffe, N. M., 1980, Brittle faults (Ramapo fault) and phylonitic ductile shear zones in the basement rocks of the Ramapo seismic zones New YOrk and New Jersey, and their relationships to current seismicity, in: Manspeizer, W. ed,, Field Studies of New Jersey geology and guide to field trips, New York State Geological Association 52nd Annual Meeting, Rutgers University, Newark, New Jersey, p. 278-311.

Rickard, M. J., and L. K. Rixon, 1983, Stress configurations in conjugate quartz-vien arrays: Journal of Structural Geology, v. 5, p. 573-578.

Roering, C., 1968, the geometrical significance of natural en-echelon crach arrays: Tectonophysics, v. 5, p.107-123.

Shainin, V. E., 1950, Conjugate sets of en-echelon tension fractures in the Athens Limestone at Riverton, Virginia: Geological Society of America Bulletin, v. 61, p. 509-517.

Wise, D. U., Dunn, D. E., Engelder, J. T., Geiser, P. A., Hatcher, R. D. , Kish, S. A.., Odom, A. L., and Schamel, S., 1984, Fault-related rocks: suggestions for terminology: Geology, v. 12, p. 91-394.

ROAD LOG FOR THE GREEN POND OUTLIER OF NEW JERSEY AND NEW YORK:
A MESOSTRUCTURAL LABORATORY

CUMMULATIVE MILEAGE	MILES FROM LAST POINT	ROUTE DESCRIPTION
0.0	0.0	Begin at Warwick, NY, Route 94 at Burger King on the south end of town. Proceed south on Route 94.
1.5	1.5	Left on Warwick 'Turnpike' at Lloyds Supermarket.
7.2	5.7	Right on Clinton Road at southern tip of Upper Greenwood Lake, NJ.
16.5	9.3	Left on Route 23 East.
18.1	1.6	Pass roadcut at top of hill.
18.6	0.5	Pass Charlotteburg Reservoir on the right and exit right at traffic light for a U-turn. Left on Route 23 westbound.
18.8	0.2	Exit right into rest area and park at far end. This is Stop 1 (two hours).

STOP 1. MESOSTRUCTURES IN THE UPPER GREEN POND CONGLOMERATE

The Green Pond Conglomerate forms the distant cliffs which probably lie unconformably on the Middle Proterozoic rocks beneath the lake. This is the eastern margin of the Green Pond outlier. Bedding dips northwest beneath the mountain. You are also located at the transition between the northern portion of the outlier defined by one large syncline and the central portion defined by three smaller wavelength anticline /syncline pairs. Superimposed on this NW dipping limb are two smaller anticline/syncline pairs that can be seen in this roadcut.

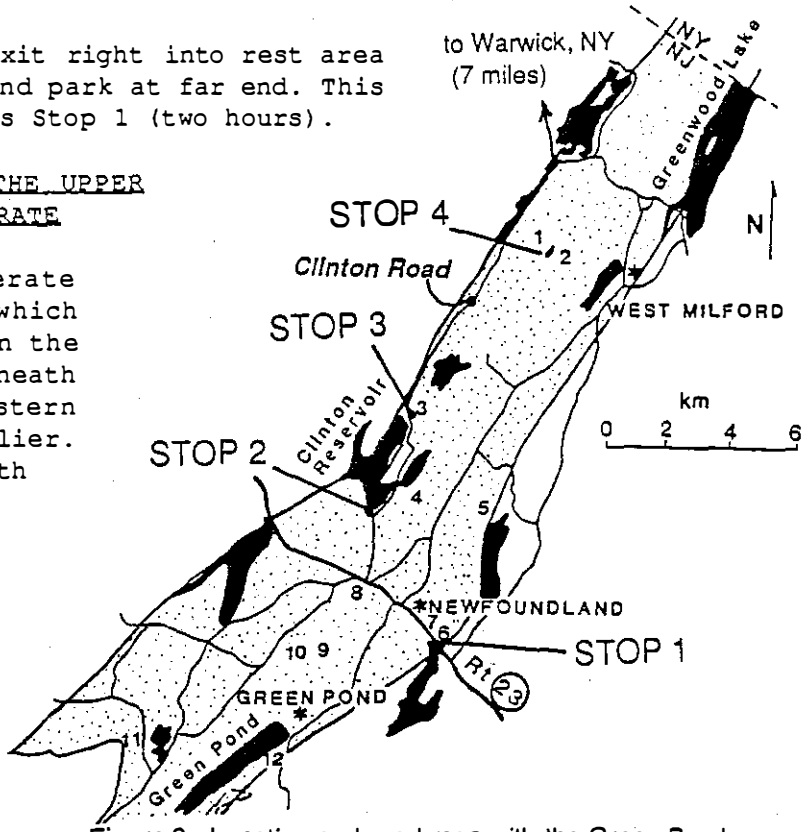

Figure 9. Location and road map with the Green Pond outlier shaded. Small number are data localities, and stop numbers are for this road log.

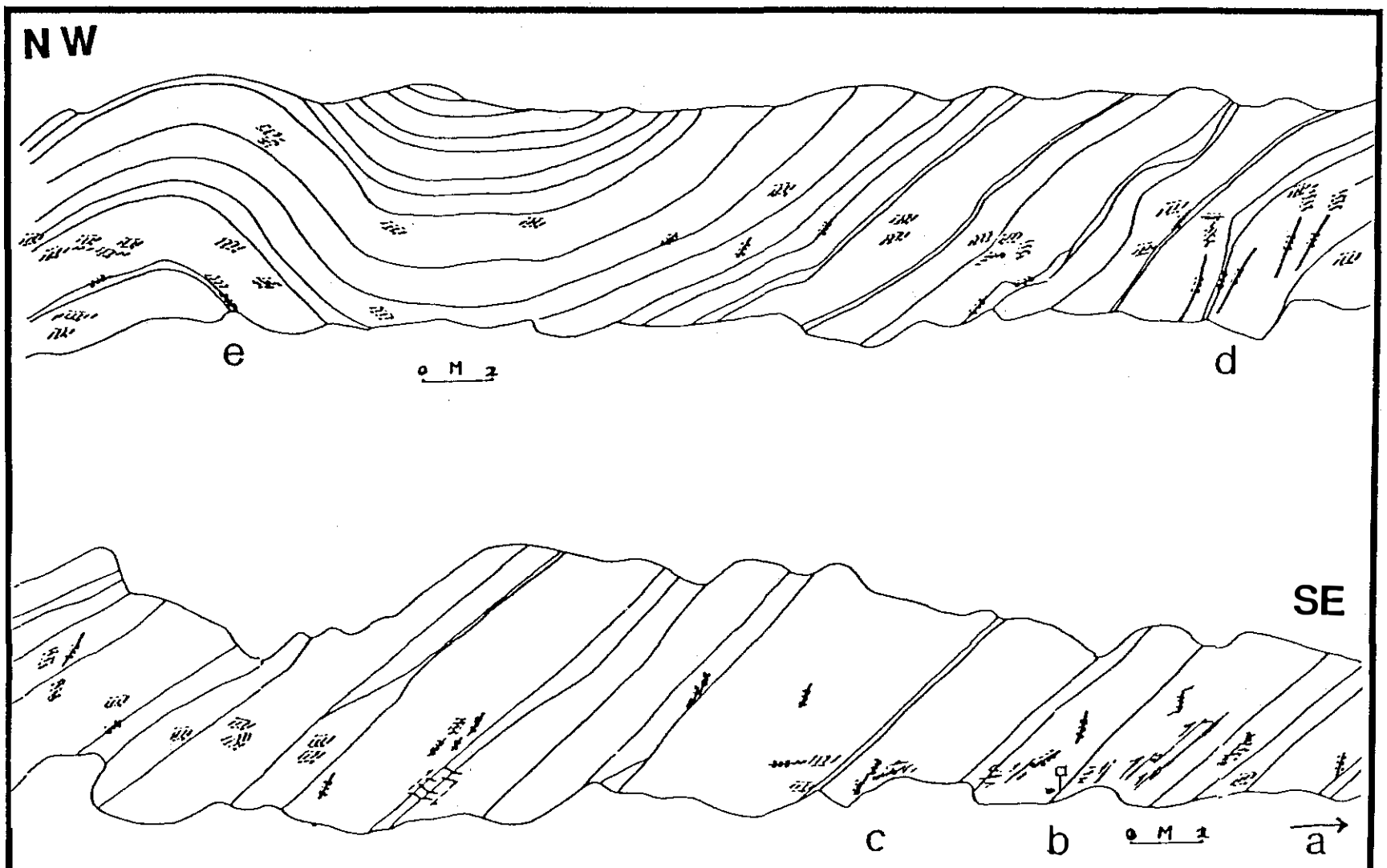

Figure 10. Sketch of the north side of the Rt. 23 outcrop (stop 1) with distribution of the EVA and SFF shown diagramatically. The bench mark and letters are reference point of interest in road log.

The purpose of this stop is to examine associations of the en echelon vein arrays, slickenfiber faults, and cleavage and to relate them to paleostress directions and progressive folding.

Walk along the west bound lane about 100 m to the north face of the exposure. Beginning at the east end of the outcrop, walk about 10 m until you see quartz veins at eye level.

a. En Echelon Vein Arrays. Several subhorizontal arrays of quartz veins occur in 'en echelon' arrangement (Fig. 11). Each array forms within a tabular shear zone and contains veins with a geometry that clearly indicates the sense of shear. In this case the top block moved westward (to the left). These features called en echelon vein arrays (EVA) have also been called tension gash arrays.

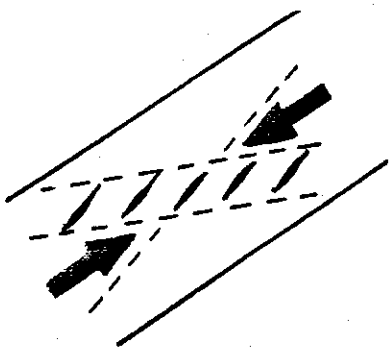

Figure 11. Illustration of how to determine the direction of maximum principal stress from a single en echelon vein array.

EVA Paleostress: The array and vein attitudes indicate (assuming type 1 geometry, see Figure 3b) that bedding parallel compression caused these particular EVA's to form. The direction of maximum compression that forms an EVA parallels the direction of greatest shortening which lies somewhere in the acute angle between the shear zone (array attitude) and a vein member (Fig.11).

Walk 30-40 m to the small Geodetic Survey sign located above a Bench Mark. See Figure 10 for location.

b. Slickenfiber Faults. Examine the many minor faults (Fig. 12) with lineations defined by mineral fibers, called slickenfiber faults (SFF's ; terminology of Wise, et al., 1985). Profiles of these features show overlapping fibers and give a sense of displacement characteristic of SFF's . Note that the quartz filled pull apart structures along some of of the SFF's give a reverse sense of displacement. The "rough-smooth" method (Durney and Ramsay, 1973) also indicates reverse displacement. The

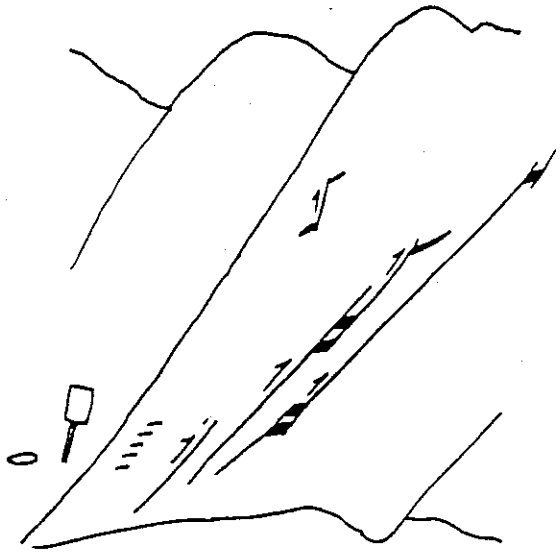

Figure 12. Field drawing showing SFF that nucleated on cross bedding. Pull aparts confirm motion inferred from the SFF fibers.

exposed footwall surface feels smooth to the hand when rubbed upwards along the surface, therefore the hanging wall moved up defining a reverse motion. The rough-smooth technique is reliable for SFF's because fibers always lie in plates that are overlapped in one direction like the shingles on a roof.

SSF Paleostress: Most SFF surfaces here developed on crossbedding surfaces dipping more steeply to the northwest than the bedding. Thus bedding parallel compression indicated by the EVA's, may also represent a conjugate shear system with SFF's following steep planes of weakness in the rocks (crossbeds oriented suitably for slip in the given stress field) and EVA's forming subhorizontal shears across rock anisotropies and in more massive rocks.

Walk 7 m west of the Bench Mark. See Figure 10 for location.

c. Conjugate EVA's and SFF's. As sketched in Figure 13, conjugate SFF's and EVA's occur in concert. A subhorizontal SFF overprints an EVA with the same sense of displacement (top block westward). This is conjugate to a steeply dipping bedding plane-SFF with veins whose displacement is top block upward to the east. These displacements are opposite but complementary such that the principal axes of shortening and compression bisects the two shears and is at a low angle to bedding. Lying in the intersection of the two shears is a quartz vein which is subparallel to the compression direction. This vein is common in conjugate EVA's and is a reliable indicator of paleostress directions.

Progressive Strain: Note the subhorizontal EVA veins in Figure 13 are sigmoidally shaped indicating progressive shear whereas, the steep EVA veins are straight, dilated, and incompletely filled with large quartz crystals (comb structure). This conjugate association can be seen in other places and may represent a slight rotation of the principal axis of compression towards the sigmoidally deformed EVA's (Fig.14). Such a rotation of the stress field, following the initial development of conjugate EVA, would substantially dilate one set of veins. This set will have straight tips which propagate at high angles to their array (synrotational EVA's of Fig. 8). The other set of veins will have curved tips that propagate at low angles to the array (antirotational EVA's of Fig. 8).

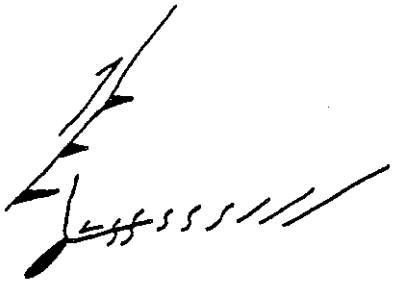

Fig. 13. Sketch of conjugate shears (Stop 1c).

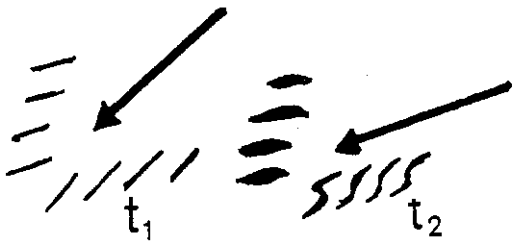

Fig. 14. 2 stage rotation (T1 and T2) for forming asymmetric EVA's.

Walk about 34 m to a position where purple rocks project slightly closer to the curb. See Figure 10 for location.

d. EVA and SFF Links. Again, SFF's occur on steep crossbeds, but this time several SFF's at eye level link up with EVA's higher in the outcrop to form a continuous shear zone with a mutual reverse sense of displacement (Figure 15). Furthermore, the same EVA's are paired with subhorizontal EVA's of the conjugate orientation. This is an outstanding association that clearly indicates the complimentary association of SFF's and EVA's in this area, and the conclusion that many of these features formed in response to maximum compression directed subparallel to bedding.

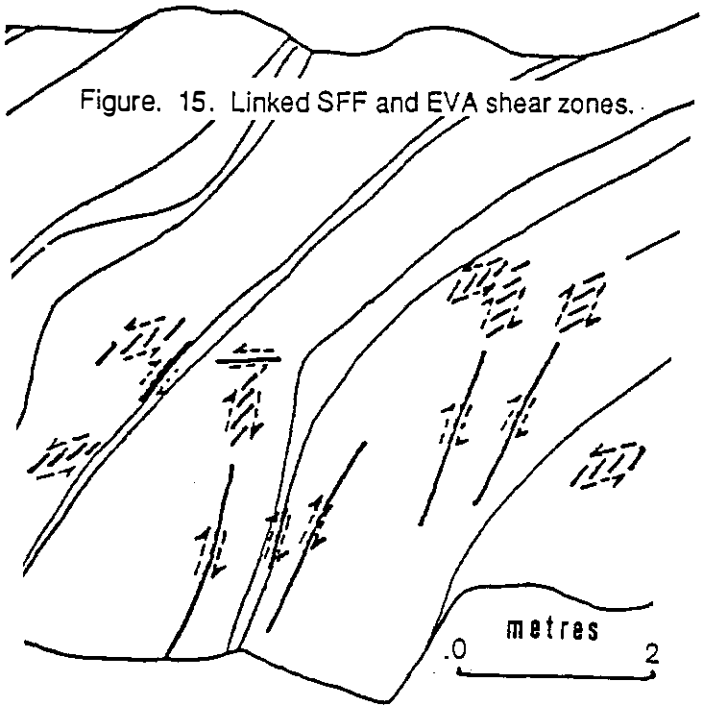

Figure. 15. Linked SFF and EVA shear zones.

Importance of microcracking: What controls whether a shear zone will develop into a SSF or EVA? Certainly planes of weakness in the rock favor SFF development, but sometimes SFF's cut across rock anisotropies. We postulate that the microcracking distribution prior to rock failure determines the thickness of the shear zone and therefore whether SFF's or EVA's will develop (Fig. 16). For example, the linked SFF and EVA shear zones at this site may reflect an incipient zone of microcracking that was narrow at the base where the SFF end developed and wider at the EVA end.

Figure 16. Sketch illustrating a possible cloud of early microcracks which may control eventual SFF or EVA geometries.

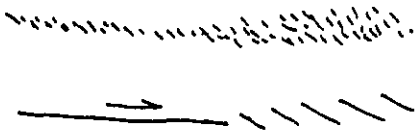

Walk about 30 m to a southeast dipping limb and the core of an anticline. See Figure 10 for location.

e. Mesostructures Record Progressive Folding History. Beginning here two anticlines and synclines can be viewed in four sections (the median exposes two sections). Veining here is profuse and complicated. Some EVA's in the hinge zone are bent or curved with pronounced sigmoidal shapes. These veins are interpreted to have been formed early and then incrimentally deformed during folding. In the median exposure (facing the west bound lane), there is a complex set of crosscutting veins that reflects rotation of the veins with respect to stresses during buckling. A late vein found here is suggestive of a late subhorizontal compression subnormal to a steep cleavage in an adjacent bed. Also in the cleaved bed (purple bed at the end of the median), is a conjugate EVA with compression bisecting the obtuse angle. Dissolution of

veins at cleavage selvages confirms that this conjugate EVA was later shortened during cleavage development. Also, the veins of the subhorizontal EVA are sigmoidally deformed while the veins of the steep EVA are comparatively straight and dilated (as at site c.). This suggests that the principal stress field rotated away from bedding parallel compression as folding progressed (model shown in Fig. 8). This deformed zone may be very near the fault tip of a buried northwest-dipping reverse fault. It also parallels a steep northwest dipping reverse fault exposed about 100 m to the northwest in the median. In addition to the fault, two anticline-syncline pairs can be seen from both traffic lanes when walking northwestward along the median.

		Return to vehicle and proceed west on Route 23.
20.6	1.8	Right onto Clinton Road.
21.8	1.2	Left on dirt road just before stream bridge and opposite old stone furnace. Proceed around the curve and up the hill for a short distance.
21.9	0.1	Park at the hilltop overlooking Clinton Reservoir and Dam. This is Stop 2.

STOP 2. MESOSTRUCTURES IN THE BELLVALE SANDSTONE

The Bellvale Sandstone floors the road shoulder. Bedding dips NNW towards the axis of the major syncline that extends northeastward into New York State. You are at a position on the fold near the hinge where bedding begins to wrap around the nose of the plunging syncline. The purposes of this stop are to examine EVA's, cleavage and their geometric relations.

Cleavages: A pronounced spaced cleavage strikes about N 80 E subparallel to bedding and a faint cleavage strikes about N 60 E subparallel to the fold axis (time permitting, cleavages and bedding attitudes are more clear at the spillway bridge on Clinton Road, northern stream bank).

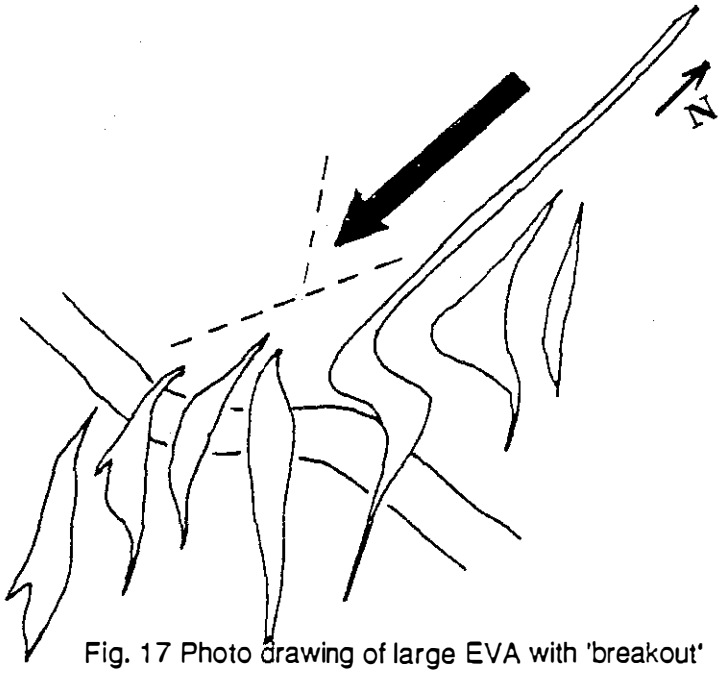

Fig. 17 Photo drawing of large EVA with 'breakout' veins paralleling the acute bisectrix. Pre-existing horizon (transverse band) is displaced sinistrally.

En Echelon Vein Arrays: A large EVA seen here indicates N-S shortening and compression (using the vein/array bisectrix rule for type 1 geometry). This stress field is roughly normal to the spaced cleavages and is postulated to represent a second discrete non-coaxial phase of deformation in the Green Pond outlier. Also note the occasional occurrance of unusually long vein tips extending beyond the EVA shear zone (Fig. 17). These veins when propagating out of the shear zone commonly curve into parallelism with the bisectrix of the vein and its array. This is the direction of the inferred maximum compression. If microcracks in the shear zone in part control vein attitudes then veins that propagate faster than others breakout of the array and may be free of the internal constraints that control intra-EVA crack tips. Thus the breakout veins are probably reasonably good indicators of the paleostress field.

Slickenfiber Faults: SSF offset some veins, most with apparent left lateral displacements. However, some of these have fibers that actually indicate dip slip motions on NW dipping surfaces.

		Return to vehicles, and drive back down the hill
22.0	0.1	Left onto Clinton Road, and over the spillway bridge, where a water fall and stream cut exposure is visible on the right.
24.2	2.2	Left into parking area for a boat landing to the Clinton Reservoir (just after the road curves to the left). Walk from the northern entrance of the parking area across Clinton Road to small cliff exposures near the road. This is Stop 3.

STOP 3. MESOSTRUCTURES IN THE LOWER SKUNNEMUNK CONGLOMERATE

You are in the same syncline as that present at Stop 2 but on the opposite limb. Beds of the lower Skunnemunk dip steeply SE towards the syncline axis. Rocks vary in color (gray, red, purple) and lithology (conglomerate, sandstone, muddy siltstone), typical of the Bellvale-Skunnemunk gradational contact. The main purposes of this stop are to: 1) see two cleavages, and 2) see unusally large EVA's that record hinge parallel compression.

Cleavage: Two spaced cleavages are visible in some of these rocks. One strikes northeastward subparallel to bedding and the fold axis, the other strikes N 85 E. They have the same general strikes as the two cleavages at Stop 2 suggesting two distinct periods of shortening.

En Echelon Vein Arrays: EVA's record a variety of paleostress directions at this site. Figure 10 shows EVA data compiled from Stops 3 and 4 (SE dipping limb only). Some EVA's on this limb of the fold record NW trending (steeply plunging) layer-parallel compression, but other indicate compression at high angles to bedding. These likely record early and late stages, respectively, of

a progressive folding history.

Some EVA's in this area record more northerly directed compression. These directions are approximately normal to the N 85 E cleavage.

Unusually large EVA's record NE-SW trending compression directed subparallel to the fold axis. They contain large gently dipping veins often dilated and incompletely filled. Veins are typically one meter long, one meter wide, and spaced up to two meters apart. They likely formed late in the folding history once the fold axis was well defined. They may be an anisotropic response to the N-S directed shortening by other EVA and compatible with the N 85 E cleavage.

Slickenfiber Faults: Most SFF's are bedding plane and cross bedding slip surfaces that record NW trending displacements that are compatible with major folding and NE trending cleavage development.

		Return to vehicles, Proceed north on Clinton Road.
28.5	4.3	Pull off along the road where the forest has been cleared for the gas pipeline. This is Stop 4 (strenuous hike to, and from, Terrace Pond of 1.4 miles round trip)

STOP 4. MESOSTRUCTURES IN THE UPPER SKUNNEMUNK CONGLOMERATE

You are located on the same SE dipping limb as at Stop 3, but in this case we are hiking up the hill to the east (up section) into the axis of the syncline. The purposes are to observe numerous SFF's, EVA's, and a distinct N 85E cross cleavage. Lock the vehicles, and hike eastward up the mountain along the right side of the pipe line clearing. Although the hike is perhaps strenuous to some, the geology and scenery (at Terrace Pond) makes this a worthwhile endeavor.

As you work your way up the ridge keep an eye out for the trail head of the Blue Dot Trail that will take us to Terrace Pond (0.3 miles up the gas line clearing). Before heading in, however, there are exposures under foot in the pipe line clearing near the trail head worth a bit of investigation.

Slickenfiber faults: The outcrops under foot in the pipe line clearing contain exposures of conjugate SFF's. Also, along the forest edge opposite the entrance to the trail is a slip surface worthy of close examination. Here, the SFF surface has two directions of fibers. Upon inspection you should be able to discern their relative timing. A N-S oriented set of fibers has been superimposed over a NW-SE oriented set, and suggests a clockwise shift in the axis of maximum compression.

En echelon vein arrays: The EVA's here largely record NW-SE trending shortening compatible with folding and most SFF's.

Now proceed into the woods on the Blue Dot Trail to Terrace Pond (0.4 miles). Along the way are a discontinous series of exposures within which various mesostructures can be examined.

Terrace Pond.

Cleavages: A distinctive spaced cleavage occurs throughout this area that trends obliquely to the fold axis at about N 80 E. It crosses both limbs and can be seen on both sides of the pond (see Figure 18 for cleavage and bedding) The far cliff descending into the pond is the opposite limb of the syncline (bedding: N 35 E, 75 NW). You are standing on the western limb that forms the west margin of the pond (bedding: N 22 E, 30 SE). The fold axis is submerged. Many mesostructures can be seen along the White Dot Trail that circles the pond. For example, on the west margin an excellent pair of intersecting conjugate EVA's record a near N-S trending compression compatible with cleavage formation in the same rocks (see Fig. 19).

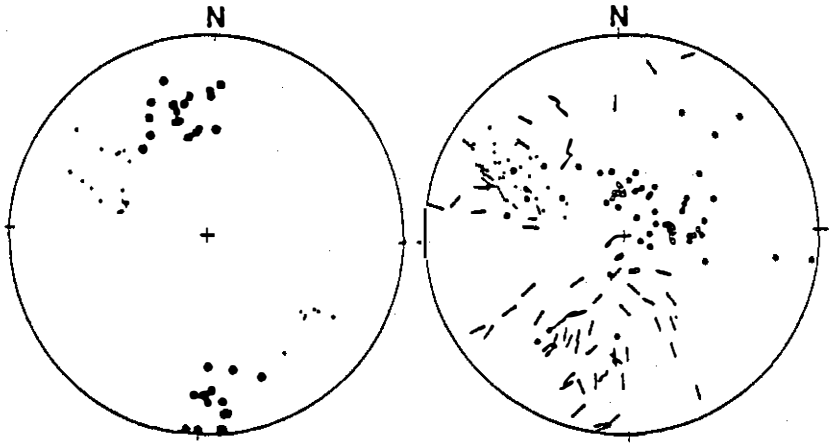

Figure 18. On the left is a stereoplot of poles to cleavage (big dots) & bedding (small dots) from Terrace Pond, and on right is a stereoplot of paleostress data from SE-dipping limbs of Stops 3 & 4. Symbols are as in Fig. 4b.

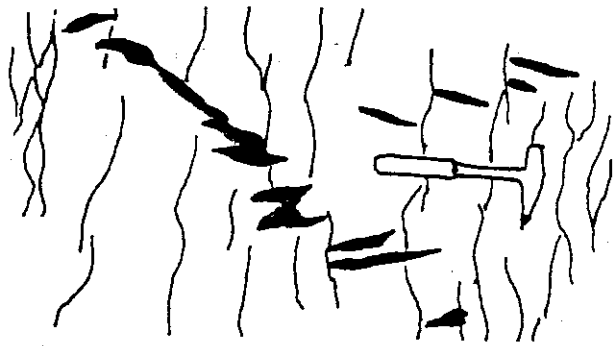

Figure 19. Sketch of field site with conjugate EVA's and spaced cleavage. Both record N-S shortening. Hammer for scale.

Field Excercise for Students. This location is an excellent choice for conducting a field-base lab in mesostructural analysis. Structure students can be taught how to recognize, measure, and interpret SFF's and EVA's along the trail on the way in to Terrace Pond. Then, working around the pond on the White Dot Trail they can collect their own data, first on the west limb, and then on the east limb. The data can be plotted later on stereonets and used for making an interpretation of the paleostress history in the area. Sample data spreadsheets, and a crib sheet for measuring EVA's are shown in Figure 20. The scenery and wilderness setting certainly adds a sense of spirit and

adventure to what might otherwise be thought of as a rather tedious excercise.

Hike back to the vehicles, retracing our route along the same trails.

		Proceed northward on Clinton Road
30.1	1.6	Turn left onto Warwick Turnpike, at Upper Greenwood Lake, N.J.
35.8	5.7	Turn right onto Route 94 at Llyods Supermarket.
37.3	1.5	Return to Burger King at Warwick, NY.

Figure 20. Procedures for the measurement of EVA

- Draw a rough map of trails, power lines, etc., and as you proceed plot your traverse so that you can locate your data collection sites.
- Find an array with at least three en echelon veins.
  Do not measure joints or isolated veins.
  Measure the EVA only if the rock appears to be firmly in place.
- At each locality measure and record onto the data sheet the following information.

1) Note the location number, the distance and direction from the previous locality, & plot the location on your field map.
2) Estimate the average vein length (roughly) for each array to be measured.
3) Take the strike and dip of a representative vein (if they are highly curved use the outer portion of a representative vein, but try not to use any vein tips that wander out of the main array).
4) Take the strike and dip of the array (usually difficult).
5) Assign a rough confidence level for each EVA measurement ; use these symbols:

good	fair	poor
+ <5°	Φ <20°	− <60°

6) Note the rock type, color, & bed thickness.
7) Take the strike and dip of bedding.
8) Take the strike and dip of cleavage (when present; and indicate cleavage type, e.g. slaty, pressure solution, etc.).
9) Sketch the geometry of the EVA & its relationships to bedding (if visible)
10) Make comments such as:
   - possible or definite conjugate EVA's
   - possibly tilted exposure
   - any association with SFF
   - any cross cutting veins, (EVA or SFF, indicate relative ages if apparent).

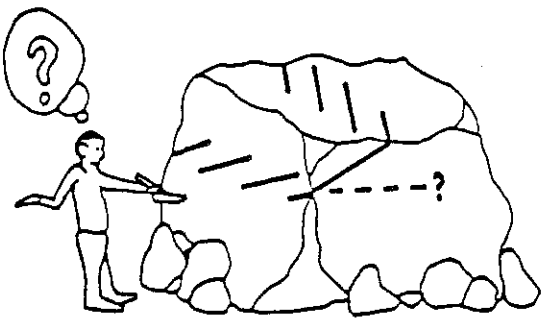

LOCATION NO.	AVG. VEIN LEN.	STRIKE & DIP OF VEIN	CONFIDENCE	STRIKE & DIP OF ARRAY	CONFIDENCE	ROCK TYPE, COLOR, THICKNESS	STRIKE & DIP OF BEDDING	STRIKE & DIP OF CLEAVAGE	CLEAVAGE TYPE	DRAWINGS

Sample data spread sheet

NOTES